J Mater Sci: Mater Med (2007) 18:1471–1479
DOI 10.1007/s10856-007-0150-1

Comparison of histomorphometrical data obtained with two different image analysis methods

Lucia Ballerini · Victoria Franke-Stenport · Gunilla Borgefors · Carina B. Johansson

Received: 17 November 2005 / Accepted: 6 April 2006 / Published online: 27 March 2007

Abstract A common way to determine tissue acceptance of biomaterials is to perform histomorphometrical analysis on histologically stained sections from retrieved samples with surrounding tissue, using various methods. The ''time and money consuming'' methods and techniques used are often ''in house standards''. We address light microscopic investigations of bone tissue reactions on un-decalcified cut and ground sections of threaded implants. In order to screen sections and generate results faster, the aim of this pilot project was to compare results generated with the in-house standard visual image analysis tool (i.e., quantifications and judgements done by the naked eye) with a custom made automatic image analysis program. The histomorphometrical bone area measurements revealed no significant differences between the methods but the results of the bony contacts varied significantly. The raw results were in relative agreement, i.e., the values from the two methods were proportional to each other: low bony contact values in the visual method corresponded to low values with the automatic method. With similar resolution images and further improvements of the automatic method this difference should become insignificant. A great advantage using the new automatic image analysis method is that it is time saving—analysis time can be significantly reduced.

L. Ballerini · C. B. Johansson (✉)
Department of Clinical Medicine/Medical Technology, Örebro University, SE 70182 Orebro, Sweden
e-mail: carina.johansson@ikm.oru.se

G. Borgefors
Centre for Image Analysis, Swedish University of Agricultural Sciences, Uppsala, Sweden

V. Franke-Stenport
Department of Prosthetic Dentistry/Dental Materials Science, Inst. of Odontology and Department of Biomaterials, Inst. of Surgical Sciences, The Sahlgrenska Academy at Göteborg University, Goteborg, Sweden

Introduction

Biomaterials research often involves in vivo tests of implants inserted into bone tissue with subsequent histomorphometrical quantifications of bone tissue reactions to the material. The animal models, the design of implants, the time of insertion, the handling of samples including laboratory techniques as well as methods and equipment used for the analysis are some factors that vary among laboratories. What is common is most likely the time it takes to perform the analysis. Equipment with more or less sophisticated image analysis tools are often used today. Briefly, while some demand much interaction (requiring the investigator to interpret and decide the findings in the interface) others may well be semi-automatic (the equipment itself ''judges the interface''). Some devices use light microscopic investigations performed ''directly in the eye-piece'' of the microscope while others have the sections presented on a screen. To the best of our knowledge, there is no ''perfect tool'' available on the market. However, it would be very interesting to find a tool that would be able to perform rapid screening and thus present reliable and instant quantitative data of tissue reactions to implants. This could eventually reduce the time of analysis as well as possible

'' operator errors'', i.e., misinterpretations that could be involved. An automatic system may not, as yet, be able to perform the delicate judging and interpretations of various important qualitative findings, but it would give the same result every time, which may not be the case for human interpretation.

When considering histomorphometrical analysis only, we know that the techniques for preparation of un-decalcified cut and ground sections with an implant in situ are very time consuming and so are the quantification methods. The differences in hardness between biomaterials and resin may often result in sections with some un-evenness between implant and bone. This artefact may lead to inappropriate measurements in the interfacial region. In the worst case, this can appear in the light microscope as a shadow effect, since the implant may be somewhat thicker than the bone tissue. To a ''biologically trained eye'' this shadow effect may not be a significant problem when analysing the sections directly in the light microscope (due to the possibility of switching between different magnification levels whilst working), but this artefact could jeopardize automatic quantifications and give false positive measurements. The entire ground section thickness varies between laboratories. While some laboratories perform quantifications of bone tissue reactions on sections more than 100 μm thick, others prefer to work with sections just 10 μm. It has been shown that the thickness of a cut and ground section is of utmost importance for obtaining reliable results and that misinterpretations arise with thicker sections (1).

The aim of the present study was to compare histomorphometrical data obtained with a routinely used light microscopical research tool involving non-automatic measurements (''visual method'') with similar data obtained by a new computerised image analysis method (''automatic method''). The main question addressed in this paper is thus: is the data obtained with the visual method in agreement with the data obtained with automatic method?

Materials and methods

Threaded titanium alloy (Ti6Al4V) implants (n = 14) (outer diameter 3.75 mm and 8 mm long) were machined, degreased and sterilised before insertion in the hind legs (tibial tuberosity region) of mature New Zealand white rabbits (n = 7). The healing time was 12 weeks. The study was approved by the local animal ethics committee at Göteborg University, Sweden.

The implants were retrieved together with surrounding bone tissue and immersed in 4% neutral buffered formaldehyde. Sample processing followed the internal guidelines of the laboratories and, in brief, this involved dehydration in ethanol and infiltration in resin to enable embedment of the samples in light curing resin. All processing of samples and sections was carried out using the Exakt equipment (Exakt Apparatebau, Germany). The cured blocks were divided in the long axis of the implants in modified band saws followed by grinding the surfaces and gluing a supporting plexiglass cover slide onto the surface. Un-decalcified cut and ground samples were processed to give 10 μm thin sections [1, 2].

The sections (Fig. 1) were histologically stained in a mixture of 1% Toluidine blue and 1% pyronin G prior to coverslipping followed by quantifications [3].

The histomorphometrical quantifications involved measurements of:

i) bone to implant contact in all available threads around the implant,
ii) bone to implant contact in the three best consecutive threads in the cortical region,
iii) bone area in all available threads around the implant,
iv) bone area in the three best consecutive inner threads in the cortical region and (Fig 8),
v) bone area in all available out-folded areas (mirror images),
vi) bone area immediately outside the three best consecutive inner threads (mirror image) (Fig 9).

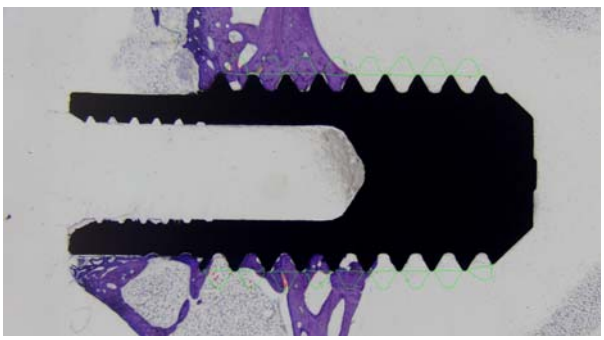

Fig. 1 This representative image demonstrates an overview of a cut and ground section. In the old, visual method one thread at a time was visualized in the eye piece of the light microscope, while in the new automatic method the entire section, with all threads, was used in the computer. The quantifications involved: bone to metal contacts (outlining the interface region), bone area in the inner threads, and the bone area immediately outside the inner threads., i.e. mirror images, the latter outlined in the figure (see also Figs 8 and 9). Staining = toluidine blue mixed in borax and pyronin G. Magnification = the distance between the thread peaks is 600 μm

Quantifications were performed by the visual method and the automatic method;

i) The visual method: all measurements were performed by one investigator, trained for several years in the biomaterials research field for histomorphometry of bone tissue reactions around implants. This person performed the analysis using the laboratory's routine equipment and standard method, i.e., in a Leitz Aristoplan light microscope, with Leitz Microvid equipment attached to the microscope and connected to a PC. The measurements were performed ''directly in the eye-piece'' of the microscope. The enlargement of the section covered one thread (i.e., the measurements were performed in one thread at a time, where the distance between the two visualized thread peaks is 600 μm).
ii) The automatic method was developed for this specific purpose, using adaptations of ''standard'' image analysis tools. Image acquisition was performed in an Olympus BX 40 light microscope connected to a microscope digital Olympus DP11 camera system. The digital colour images were 1368×1712 pixel matrices with a resolution of approximately 14×14 μm, which means that each image contains an entire section. The images contain the entire section and the measurements were automatically taken in all threads at the same time (resulting in much lower resolution than that used in the visual method). The automatic method is summarized below and later described in detail.

1. Pre-processing: the acquired image is treated to reduce the effect of undesired imperfections of the image acquisition in order to improve the results of the analysis.
2. Segmentation: this is the most important, but also often the most difficult task in image analysis. The aim is to identify and outline the individual objects in the image.
3. Region of interest (ROI) selection: select the regions where measurements should be performed.
4. Measurements: Measure areas and lengths of the interesting objects in the ROIs.

Image pre-processing

The image background is usually non-uniform. This is caused by uneven illumination of the field of view of the microscope, i.e., images are lighter in the mid/central part and darker close to the borders. Although this has limited impact on the visual method, it severely complicates automatic image segmentation. A possible solution could be to acquire a background image (without the section). When this image is not available the background can be automatically estimated, which was done here [4]. The algorithm works by iteratively improving the estimate of the background of the image. The background is assumed to be smooth and slowly varying and can therefore be modelled by spline functions. The background image is then subtracted from the original image to produce a background compensated image. The original colour images were split into their Red, Green and Blue components and the background correction algorithm was applied independently to each component. The following parameters were used: kernel size = 64, maximum number of iterations = 30, offset = 200.

The next step is to estimate and correct the shadow between implant and bone. As described in the introduction, this effect is due to the differences in surface height caused by different hardnesses of biomaterial and bone/resin. A specific method had to be developed and applied in order to avoid incorrect segmentation and therefore inappropriate measurements in the interfacial region. The shadow was estimated using only the intensity component (the average of the Red, Green, and Blue components) of the images. A plot of the shadow variation was obtained by averaging the intensity values against their distance from the implant [4]. The 2nd order polynomial coefficients were estimated and used to correct the shadow in the whole image. Figures 2 and 3

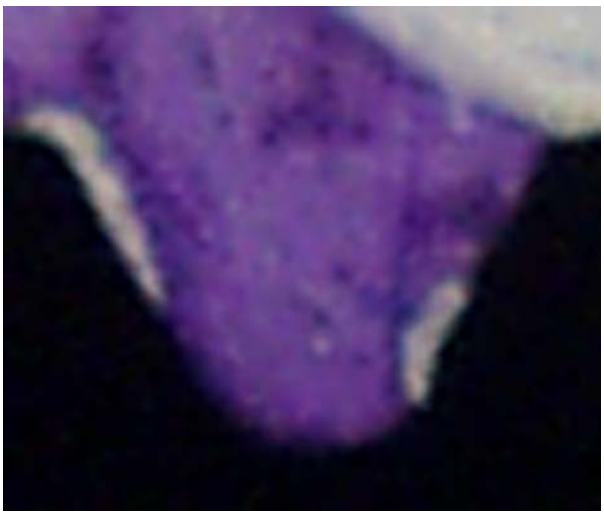

Fig. 2 Image of a thread before (2) and after (3) the correction of the shadow in the interfacial region. The shadow has been estimated by averaging the intensity variation and plotting them vs. the distance from the implant

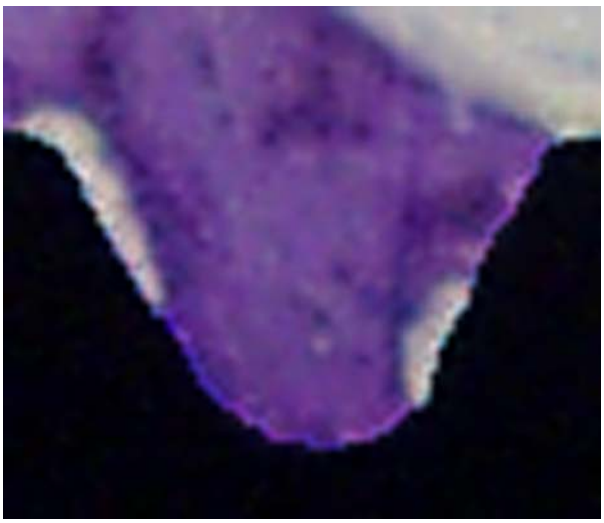

Fig. 3 Image of a thread before (2) and after (3) the correction of the shadow in the interfacial region. The shadow has been estimated by averaging the intensity variation and plotting them vs. the distance from the implant

show a detail of a thread before and after shadow correction.

Image segmentation

The ''fuzzy c-means clustering'' (FCM) algorithm, with the colour components of each pixel used as features, was used to segment the images. This algorithm is an unsupervised fuzzy clustering technique widely used in automatic image segmentation [5].

The standard FCM algorithm is based on the minimization of the following objective function:

$$J_m(U,V) = \sum_{i=1}^{c}\sum_{k=1}^{n} u_{ik}^{m}\|x_k - v_i\|$$

where x_1, x_2, ..., x_n are n data sample vectors; $V = \{v_1, v_2, , ...,v_c\}$ are cluster centres; $U = [u_{ik}]$ is a $c \times n$ matrix, where u_{ik} is the ith membership value of the kth imput sample x_k such that $\sum_{i=0}^{c} u_{ik} = 1$;$m \in [1, \infty)$ is an exponent weight factor that determines the amount of ''fuzziness'' in the resulting classification.

The method is iterative and consists of finding the optimal cluster centres (v_i) in feature space, and assigning to each pixel (x_k) of the image a membership value (u_{ik}), ranging between 0 and 1, measuring how much the pixel belongs to a particular cluster.

Instead of the standard FCM we used a new clustering algorithm that combines the FCM with a genetic algorithm [6]. We also modified the objective function of the FCM to take into account the spatial information of the image data and the intensity

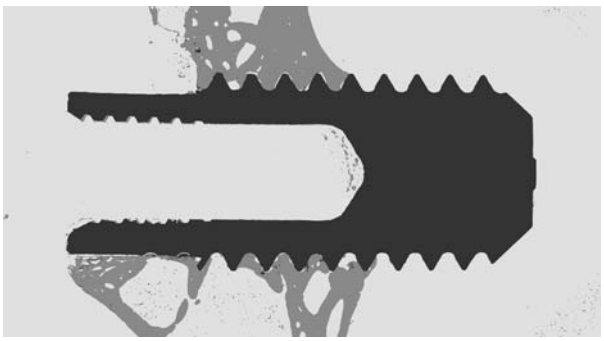

Fig. 4 Segmented image: the dark grey region corresponds to the implant, light grey areas to bone—all other pixels are white

inhomogeneities. A more detailed description is presented in Ballerini et al. [6]. The number of clusters was set to three, which corresponds to segmenting the images into three classes: implant (very dark pixels), bone (bluish pixels), and soft tissue (light pixels).

The major drawback of this algorithm is the long execution time. In order to speed up the algorithm, the cluster centres were calculated from sub-sampled (sub-sampling factor = 8) images, i.e., only a reduced number of pixels. Membership values were then calculated for all the pixels in the images. Figure 4 illustrates a segmented image.

Region of interest selection

All threads were automatically selected using the following procedure: The convex hull of the implant, i.e., the smallest convex polygon containing this region was computed, and then the convex deficiencies that correspond to threads were identified [7]. The area inside the hollow screw also formally belongs to the convex deficiency, but since this is not of interest it was removed.

Some adjacent threads will be linked and since we were interested in each thread by itself these links have to be dismantled so that each thread comprises a single region. To do this, first a distance transform [8] was computed in the convex deficiency from its border and then the watershed algorithm [9] was applied to the resulting distance image. This nicely splits any connected threads, without affecting any correctly segmented threads. Figures 5, 6 and 7 illustrate the method.

In addition to measurements in the thread regions, the aim was also to measure in non-affected areas of the same size. These areas are defined by ''folding out'' (mirroring) the thread regions into the surrounding tissue. The mirror areas were computed by using an affine transform that flips each thread region through

Fig. 5 This figure illustrates the watershed algorithm applied to a distance transform. An image of the regionalization of three linked threads (shown in Fig. 5), a distance transform of them (shown in Fig. 6), the resulting regions after the watershed algorithm applied to the distance transform (shown in Fig. 7)

Fig. 6 A distance transform of them

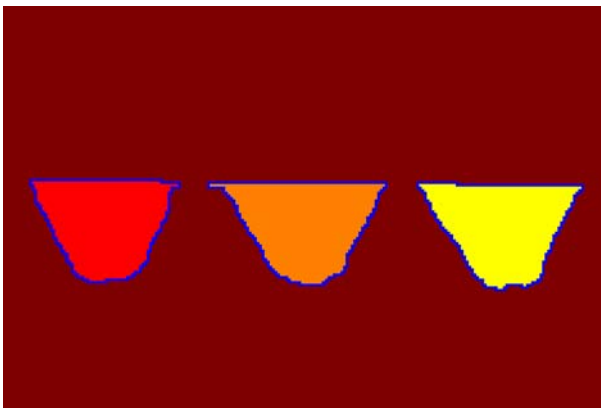

Fig. 7 The resulting regions after the watershed algorithm applied to the distance transform

its closing line. The points used by the affine transform are the end points of the thread closing line and its centroid. The end points are fixed while the centroids of the mirror regions are placed on a line perpendicular to the closing line and the same distance from it as the thread centroid. Mirror regions have the same shape and area as their corresponding thread regions (Figures 8 and 9).

Measurements

The percentage η of bone area has been computed as:

$$\eta = \frac{\int\int f_{bone}(x,y)\mathrm{d}x\mathrm{d}y}{\int\int \mathrm{d}x\mathrm{d}y} \times 100$$

where $f_{bone}\ (x,\ y)$ is the binary segmentation obtained as:

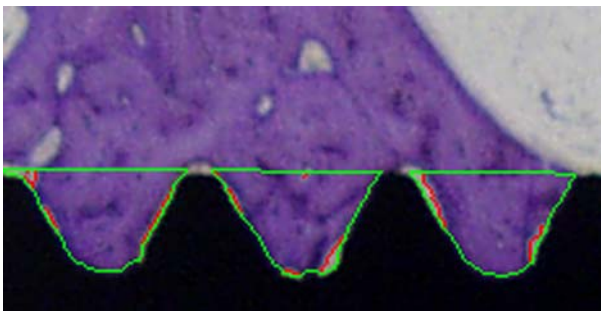

Fig. 8 Detail images with selected inner threads. The contours of the regions of interest, i.e., where we performed measurements, are highlighted in green. The contours of the bone/not-bone areas are outlined in red

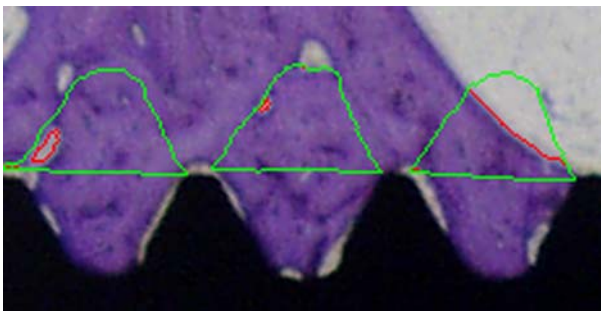

Fig. 9 Detail images with selected mirror regions. The contours of the regions of interest, i.e,. where we performed measurements, are highlighted in green. The contours of the bone/not-bone areas are outlined in red

$$f_{bone}(x,y) = \begin{cases} 1 & if \quad f(x,y) \in \text{“}bone\text{”} \\ 0 & otherwise \end{cases}$$

The existence interval of all the integrals are the selected regions as described in the previous section.

The percentage of contact (length) has been computed in a very similar way, by restricting the integration to a very narrow area (ideally one pixel thin), very close to the implant border.

Implementation

The automatic method has been implemented using Matlab. A user friendly interface has also been developed, to visualize intermediate and final results and to allow interaction by the user (some small manual adjustments are sometimes necessary). Here, manual corrections were done in a few cases, i.e., to remove small dots from the segmentation procedure (probably due to noise), or to correct the thread selection in the case of broken threads.

The time to analyse each image is less than 1 minute (including the visualization).

Statistics

The Mann Whitney U-test was used for comparisons of the mean values from each implant measured by the visual method to the mean values of the measurements of the same section using the automatic method.

Results

Predicted results from the two methods—assuming that everything worked as expected—were that area measurements should be about the same, but that bone contact (length) would be overestimated in the automatic method—were obtained. This is most probably due to the lower resolution and the implant shadow effect which both would lead to overestimation. However, trends should be similar, so that the rank order of the samples should be about the same in both cases. If so, the scale or offset differences can be compensated for or adjusted.

In fact, the results obtained followed these predictions quite well. The raw values obtained with the two methods were in agreement; i.e., low values from the visual method corresponded to low values from the automatic method. Similar trends were also present for high numbers. By ranking the data from the lowest to the highest number, a high correlation could be observed between the methods used, both for bony contacts and for bone area measurements (Figures 10 and 11).

Considering the raw numbers of the histomorphometrical data, five of the six *mean values* obtained with the visual method were lower than with the automatic method. In this one exception similar numbers were obtained (67% in both cases). The *median values* were the same for both methods in three of the six cases. The other three *median values* were higher for the automatic method compared to the visual one.

Statistically significant differences were obtained in bony contact measurements; for all threads ($p = 0.000$) and for the three best consecutive threads ($p = 0.000$). There were no statistically significant differences between the various bone area parameters.

The relationship between the *mean and median bony contact* lengths in all threads was 1:1.72 by the visual method and 1:1.66 by the automatic method.

Similar comparisons of the *bony contacts in the three best consecutive threads* were 1:1.55 and 1:1.50, respectively. For the *area* measurements the relation of the *mean* values between the visual and automatic methods varied, but was 1:1.13 at the most. The relations between the visual and automatic methods for the *median area* in all threads, all mirror regions, and the three best mirror regions, were all 1:1. Table 1 summarizes the data from all measurements and the statistical comparisons.

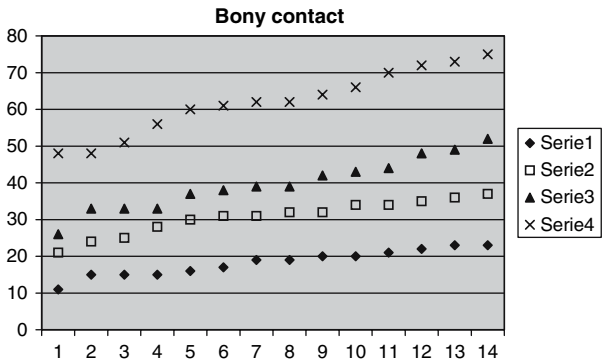

Fig. 10 This graph illustrates ranked bony contact data, measured in all threads and in the three best consecutive cortical threads, using the two methods. It is obvious that there is a strong correlation between them. Series 1 = all threads, old visual method. Series 2 = all threads, new automatic method. Series 3 = selected three best consecutive threads in the cortical region, visual method. Series 4 = selected three best consecutive threads in the cortical region, automatic method

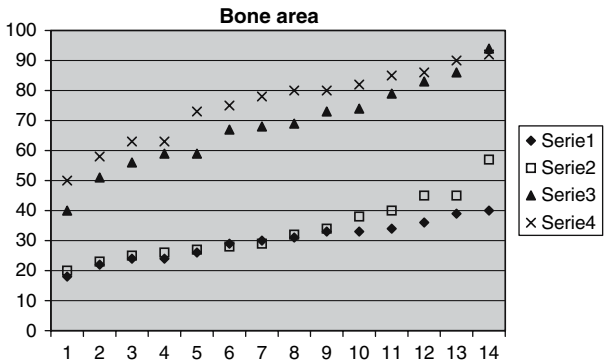

Fig. 11 This graph illustrates bone area data, measured in all threads and in the three best consecutive cortical threads, with the two methods. There is a strong correlation between the two methods used. Series 1 = all threads, old visual method. Series 2 = all threads, new automatic method. Series 3 = selected three best consecutive threads in the cortical region, visual method. Series 4 = selected three best consecutive threads in the cortical region, automatic method

Discussion

One of the ''major problems'' encountered was the preparation of high contrast digital images. Once this was achieved as well as the existing equipment

Table 1 Summary of mean and median values, standard deviation (±) and range from the two different methods used, i.e. the old visual method and the new automatic method

n = 14 observations	OLD visual method	NEW automatic method	Statistics	Relation Old:New
BMC all threads				
Mean	18 ± 4 (11–24)	31 ± 5 (21–37)	p = 0.000	1:1.72
Median	19	31.5		1:1.66
BMC 3 best				
Mean	40 ± 7 (26–52)	62 ± 9 (48–75)	p = 0.000	1:1.55
Median	39	62		1:1.50
Bone area all threads				
Mean	30 ± 6 (18–40)	34 ± 10 (20–57)	p = 0.490	1:1.13
Median	30.5	30.5		1:1
Bone area 3 best				
Mean	68 ± 15 (40–94)	75 ± 13 (50–92)	p = 0.198	1:1.10
Median	68.5	79		1:1.15
Mirror image all				
Mean	26 ± 8 (11–37)	29 ± 8 (14–47)	p = 0.461	1:1.12
Median	28.5	28.5		1:1
Mirror image 3 best				
Mean	67 ± 15 (30–95)	67 ± 16 (39–96)	p = 0.495	1:1
Median	67	67		1:1

BMC all threads = bony contact in all threads around the implant

BMC 3 best = bony contact in the three best consecutive threads in the cortical region

Bone area all threads = bone area in all inner threads around the entire implant

Bone area 3 best = bone area in the three best consecutive threads in the cortical region

Mirror image all = bone area in all out-folded mirror image threads

Mirror image 3 best = bone area in the three best consecutive threads in the cortical region (immediately outside the three best inner threads)

For statistical comparisons between data obtained by the visual and automatic methods the Statistics = Mann Whitney U-test was used. The last column depicts the relation between the data obtained by the visual and automatic methods, respectively

allowed, the process of developing the computer algorithms could start. Here, one may argue that even better base line pictures could be prepared in addition to even better qualitative sections to start with. However, as mentioned earlier, the occasional shadow effects do not jeopardize the overall outcome of histomorhometry with the standard visual method. Even with these limitations, this pilot study comparing the new automatic method with the existing technique has been encouraging.

The study has shown that it is possible to obtain similar measurements of bone area around implants with the two different methods. However, automatically quantifying the interface region with the images and automatic algorithms used here is difficult.

Several questions may arise; among them are: what parameters are most relevant/reliable in the present paper? What measures are ''true'' results? What percentage differences between the two methods are acceptable?

First, there is no consensus or proven data as to what the bony contact percentage should be and thus it is not possible to refer to ''gold standard'' data for an implant to be properly integrated. This matter was examined more closely in the thesis by Bolind 2004 [10], who investigated the bone integration of 606 retrieved human oral implants of various designs. Bone is constantly undergoing remodelling. Biomaterials researchers would assert that the data obtained by our routine tool is the ''true data''. Quantitative research data collected and compared internally over several years have shown data reliability and operator insensitivity [1, 10, 11]. One may argue that histomorphometry is most often conducted on one section only and thus may not be in agreement with the reality. This may be true albeit one very important matter, that seldom is discussed, is that one should work on thin sections. This is important in avoiding overestimations. While some laboratories work with sections several hundred micrometers thick, resulting in great (but false positive) integration, others prefer thin sections (10–15 μm) in order to avoid overestimations. In this study exactly the same sections were analysed, with two different methods.

There may be several reasons for the differences obtained with the two methods. First, this variance may be due to differences in magnification levels used. While one thread was measured at a time in the light microscope (visual method) the entire implant was visualized in one image in the automatic method. This

low magnification level cannot be used in the light microscope—the resolution would be dull and it will be impossible to judge the interface region. Second, the shadow effect visible on a few sections most probably resulted in higher percentages of bony contact with the automatic method. While a trained eye can judge the content of the tissue in the interface, even if a shadow effect is present or if the section is somewhat overstained, this cannot be judged by automatic measurements: the artefact will automatically be measured as bony contact.

It may be argued that other staining methods might enable automatic image analysis more accurately. However, for this study all samples were stained with the same method, which allows a distinction between old and new bone (pale- and dark-purple stain, respectively) while soft tissue is stained blue. As mentioned earlier, there is no consensus regarding the ''true'' percentage of integration of implants. Several studies have shown that implant integration increases with time but no-one can tell exactly what the ''true'' contact should be. From internal data and experience, we know that an implant that demonstrated high removal torques also demonstrates a high percentage of bony contact. Moreover, the bone to implant contact calculated in all threads is about half that measured in the three best consecutive threads. This was also shown in the present paper; 18% bony contact in all threads and 40% in the three best consecutive threads when measured with the visual method. Comparative numbers obtained with the automatic method were 31% and 62%, respectively.

Despite the differences observed in this investigation we believe that further work on the automatic program is warranted. An image analysis program allowing user interaction to make corrections of the automatic method's errors will most probably result in contact data closer to that obtained in the light microscope. Moreover, reduced analysis time will be greatly beneficial. The analysis time of one section only, using the visual method, is about 1 h. We estimate this could be reduced by more than 50% with improved sample preparation and image capture.

It can be argued that one disadvantage with the present study is that the measurements were not performed on the same images but at different magnifications. The visual method requires decisions from the operator in terms of what to include and measure, whereas the automatic method cannot be influenced by the operator at all. Despite this, the area measurements are in agreement for mean and median values as well as the rankings between the two methods. The reasons for significant differences in bony contact measurements are most probably low resolution, shadow effects, and possibly a too simple segmentation algorithm. The gap between bone and implant can be very narrow and when the resolution is too low, the gap is simply not detected, either visually or automatically. All measurements for the new automatic method have been done in one set of images having the same pixel resolution. We have shown that the ranking of the samples is the same as for the old manual method but that the actual measurements for contact are too large. In the future it will be necessary to test the method (or improved versions of it) on sets of digital images of different resolutions, to find out if the overestimation is a systematic error of the new automatic method or if it is—as we suspect—highly dependent on the pixel resolution. In any case, it will be possible to introduce a resolution dependent correction factor that makes the results of the new method more similar to the old one. In fact, it may be preferable to use a low resolution, as in the present test set, with a correction factor, since using a much higher resolution will necessitate many more images per sample. We consider the work done so far as a strong indication that automatic image processing can be used in this application, rather than as a finished measurement tool. The first question when we started this pilot study was whether a new image analysis tool could speed up the analysis and achieve comparable results to the existing method—and the answer is ''yes''.

Acknowledgements Research technicians Petra Johansson and Maria Hoffman, Department of Biomaterials/Handicap Research, Göteborg University, are greatly acknowledged for their skill in the cutting and grinding- and image acquisition techniques. Dr. Joakim Lindblad, Centre for Image Analysis, Uppsala, is gladly acknowledged for sharing his algorithms and for very fruitful suggestions. This work was supported by grants from the Swedish Research Council, no 621-2005-3402.

References

1. C. B. JOHANSSON and P. MORBERG, *Biomaterials*. **16** (1995) 91
2. C. B. JOHANSSON, On tissue reactions to metal implants. *PhD. Thesis*, University of Göteborg, Biomaterials Group / Department of Handicap Research, Göteborg, Sweden (1991)
3. K. DONATH, *Der Präparator* **34** (1988) 197
4. J. LINDBLAD and E. BENGTSSON, in Proceedings of the 12th SCIA *Scandinavian Conference on Image Analysis*, Norway, June 2001, edited by I. Austvoll (NOBIM, 2001), p. 264
5. J. C. BEZDEK and R. J. HATHAWAY, in Proceedings of the 1st Institute of Electrical and Electronics Engineers, IEEE, Conf. on Evolutionary Computation, June 1994; edited by Z. Michalewicz et al. (IEEE, Piscataway, NJ, 1994) p. 589.

6. L. BALLERINI, L. BOCCHI and C. B. JOHANSSON, in Proceedings Application of Evolutionary Computation, LNCS 3005, 260-269, Portugal 2004
7. R. C. GONZALEZ and R. E. WOODS, in ''Digital image processing'' (2nd edn. Prentice Hall, Upper Saddle River, New Jersey, 2001) p. 649
8. G. BORGEFORS, *Comput. Vision. Graph.* **34** (1986) 344
9. L. VINCENT and P. SOILLE, *Institute of Electrical and Electronics Engineers, IEEE. Trans. Pattern Recognit. Mach. Intel.* **13** (1991) 583
10. P. BOLIND, On 606 retrieved oral and craniofacial implants. An analysis of consecutively received human specimens. *PhD. Thesis*, University of Göteborg, Department of Biomaterials /Handicap Research, Göteborg, Sweden (2004)
11. L.V. CARLSSON, On the development of a new concept for orthopaedic implant fixation. *PhD Thesis*, University of Göteborg, Biomaterials Group, Department of Handicap Research, Göteborg, Sweden (1989)